MRI and MRS on preserved samples as a tool in fish ecology

Christian Bock*, Felizitas C. Wermter, Katja Mintenbeck

Alfred Wegener Institute Helmholtz Centre for Polar and Marine Research, Bremerhaven, Germany

*Corresponding author:

Dr. Christian Bock

Integrative Ecophysiology

Alfred Wegener Institute Helmholtz Centre for Polar and Marine Research

Am Handelshafen 12

27570 Bremerhaven, Germany

Tel.: 49(471)4831-1288

E-mail: Christian.Bock@awi.de

Keywords: Magnetic resonance imaging, NMR spectroscopy, preserved samples, formalin, *Pleuragramma antarctica*, lipids

Short Title: MRI and MRS as tools in fish ecology

Abstract

Magnetic Resonance Imaging (MRI) and Magnetic Resonance Spectroscopy (MRS) gain increasing attention and importance as a tool in marine ecology. So far, studies were largely limited to morphological studies, e.g. for the creation of digital libraries. Here, the utility of MRI and MRS for ecologists is tested and exemplified using formalin preserved samples of the Antarctic silverfish, *Pleuragramma antarctica*. As this species lacks a swim bladder, buoyancy is attained by the deposition of large amounts of lipids that are mainly stored in subcutaneous and intermuscular lipid sacs. In this study MRI and MRS are not only used to study internal morphology, but additionally to investigate functional morphology and to measure parameters of high ecological interest. The data are compared with literature data obtained by means of traditional ecological methods.

The results from this study show that MR scans are not only an alternative to histological sections (as shown before), but even allow the visualization of particular features in delicate soft tissues, such as *Pleuragramma*'s lipid sacs. 3D rendering techniques proved to be a useful tool to study organ volumes and lipid content, which usually requires laborious chemical lipid extraction and analysis. Moreover, the application of MRS even allows for an analysis of lipids and fatty acids within lipid sacs, which wouldn't be possible using destructive methods. MRI and MRS, in particular when used in combination, have the capacity to provide useful data on parameters of high ecological relevance and thus have proven to be a highly valuable addition, if not alternative, to the classical methods.

Introduction

Modern imaging modalities like Magnetic Resonance Imaging (MRI) and Computed Tomography (CT) are increasingly gaining attention in the field of zoology, in particular for morphological studies [1, 2, 3]. These non-invasive imaging techniques can easily picture the whole body of organisms in 3-dimensional (3D) digital data without the need for dissection. Supported by imaging graphic software tools, the data sets can be used to create anatomical and morphological 3D models discriminating between skeleton and organs or displaying the connectivity of, e.g., the entire cardiovascular system. Recently, MRI and CT have been successfully applied to create digital atlantes (e.g. of brains [4]) and libraries to document and store anatomical and morphological data of specimen from Natural Museums' collections, and to make these data available online for everyone (see www.digitalfishlibrary.org; [5]).

The main difference of MRI compared to other non-invasive imaging techniques is its excellent soft tissue contrast that allows detecting and illustrating structures, which are hard to unveil with classical dissection techniques [e.g. 6, 7]. The image contrast can be easily modified by running specific MRI sequences to produce a distinct discrimination between particular organs or other specific internal structures. In most tissues the contrast of MR images is primarily based on magnetic properties of water-bound hydrogen. However, in lipid-rich tissues lipid-bound hydrogen atoms significantly contributes to the image contrast, which can be utilized to image lipid-rich tissues and structures in specific body parts [e.g. 8]. The MRI, moreover, can be used in combination with Nuclear Magnetic Resonance Spectroscopy (NMR, MRS) to get localized and analytical information on, e.g., specific

65 metabolites or lipid composition of organs and body structures. This approach has resulted
66 in a multitude of applications of *in vivo* MRI and MRS in animals (for review see e.g. [9, 10]).

67 However, alive animals for such studies are not always available. In these cases, preserved
68 samples, either frozen or chemically preserved, may be studied instead. The most common
69 chemicals used for sample preservation and long-term storage are ethanol and formalin. In
70 particular formalin preservation has some clear advantages regarding tissue integrity of a
71 sample or animal compared to freezing or the use of fresh tissues: fragile structures are not
72 damaged by forming ice crystals and no water-loss occurs due to post-mortem cell-
73 degradation or warming. Chemically preserved samples are frequently available in the
74 collections of museums, research institutes or universities. Often, these collections even
75 include rare and/or highly valuable animals for which analyses of, e.g., tissue composition or
76 internal structure using traditional destructive methods is not an option to be considered.
77 For such samples or animals, non-invasive MRI and MRS represent perfect tools to study
78 their internal structure without any damage.

79 Compared to the variety of *in vivo* applications, however, the applications of MRI to
80 chemically preserved animals so far has been largely limited to general anatomical and
81 morphological studies, such as the work done in the framework of the Digital Fish Library [5].

82 Here, we intent to move beyond the pure record and representation of general anatomy and
83 morphology and to open these tools for ecological research. We extend the basic
84 morphological approach and present a protocol containing standard MR imaging sequences
85 in combination with MRS for studies on the structure and function of lipid-rich tissues
86 (functional morphological MR) in preserved organisms. This protocol is simple to apply even
87 for the non-expert MR user and demonstrated here using preserved samples of an Antarctic
88 fish as an example.

The Antarctic silverfish, *Pleuragramma antarctica* Boulenger, 1902 is one of the few truly pelagic fish species inhabiting high Antarctic waters and represents a major trophic link in the food web. As it is extremely difficult, if not almost impossible, to catch this fragile fish alive, studies usually have to rely on preserved samples. Structural analyses of this species are largely limited to histological studies of transverse tissue sections [e.g. 11,12,13]. Despite the lack of a swim bladder, *Pleuragramma* is almost neutrally buoyant; the lack of a swim bladder is mainly compensated by a reduced and low ossified bone mass (skeleton) and by large lipid deposits [11, 14, 15, 16]. Fish have unconstricted vertebrae and a persistent notochord filling the hollow centra of adult vertebrae [14, 17]. The lipids are mainly stored in intermuscular and subcutaneous lipid sacs [11, 14], which is a rather rare feature in fish. Whether the functional role of these lipids is exclusively limited to buoyancy, however, is still under debate [18].

In this study, we test for the capacity of MRI and MRS technologies to address and study ecologically relevant issues and features of fish species, such as *Pleuragramma*, when applied to preserved animals. As the lipid storage system in this fish species is very particular, we not only investigate the general anatomy and the potential to determine organ volumes, but also focus on the distribution and structure of the lipid sacs and the possibility to analyze the lipid composition. As investigating such measures of ecological interests using traditional methods (e.g., histological sections, chemical lipid extractions and analysis) is very time consuming and destructive, the modern tools used in this study might provide a useful addition or even alternative to draw a comprehensive ecological picture of a fish species. This non-invasive approach might prove particularly valuable for studying rare or highly valuable species.

Materials and Methods

Animal sampling

Individuals of adult *Pleuragramma* were taken in the western Weddell Sea, east off the Antarctic Peninsula (south of 60°S) during the RV Polarstern expedition ANT XXVII-3 in 2011 [19]. Fish were caught between 64°47,00'S / 60°23,65'W and 65°31,68'S / 61°33,13'W by means of a standard bottom trawl and a bentho-pelagic net. The sampling of fish was conducted according to the ethics and guidelines of the German law, and approved by the Federal Environment Agency (FEA; Umweltbundesamt, UBA, Wörlitzer Platz 1, 06844 Dessau-Roßlau), reference number I 3.5 - 94003-3/253, on February 1st 2011. Individuals were fixed in 10% formalin buffered with borax (sodium tetraborate) for preservation. To exemplify the capacities of MRI and MRS, individual animals were randomly chosen from the bulk of samples.

MR imaging and spectroscopy

Directly prior to MR scanning, individual fish were carefully removed from formalin to determine weight and standard length (SL, cm). Subsequently, the specimen was placed between two wooden skewers within a Perspex chamber to hold the fish in an upright position without damaging the skin. The Perspex chamber containing the fish was then positioned inside the magnet. All MRI and MRS studies were performed in a Bruker 4.7T magnet equipped with Avance III electronics. For high resolution MRI and MRS a 200mT/m gradient coil insert (BGU 12) together with an 8 cm ^{1}H-birdcage resonator (Bruker Biospin, Germany) was used. Whole body analyses (e.g. total lipid content) were conducted using the standard 50mT/m gradient coil (BGU 26) together with a 20 cm ^{1}H-birdcage resonator

(Bruker Biospin, Germany). Data acquisition and recording were carried out with ParaVision 5.1 (Bruker Biospin, Germany).

Functional morphological MR

Modified Driven Equilibrium Fourier Transform (MDEFT) imaging, as recommended for morphological MRIs [3], was used here to study the internal anatomy of preserved fish. Using a MDEFT sequence protocol from the ParaVision software, the general internal anatomy of a fish was investigated (2D) and its total body as well as stomach volume was determined (3D).

Prior to imaging, field homogeneity was optimized using an automated shim routine of the ParaVision software. The optimal morphological contrast was achieved using a fat suppression with a Gaussian pulse (700 Hz bandwidth). Parameters were as follows: Echo time TE = 7.59 ms, Echo repetition time TER = 21.16 ms, segments= 8, segment repetition time= 3353.75 ms, segmentation duration 1354.24 ms, number of averages: 64, 90° sinc10H pulse of 2 ms length, matrix size: 512x512, Field of view FOV 60x60 mm, 26 slices, slice thickness 0.5 mm, maximum achievable resolution 0.117x0.117 mm/pixel. The total acquisition time varied according to the number of averages from 5 min for an overview image for the positioning of the voxels used for localized ^{1}H-NMR spectroscopy up to 12h 24 min for high-resolution images of the lipid sacs.

All images were post processed using MeVisLab (MeVis, Germany); to determine total body and organ volumes, the 3D data were processed with the modules ‘region growing’ and ‘volume rendering’. The stomach was separated from the surrounding tissue with the selection of a region of interest (ROI). To test whether fish volume data can be used as an

159 equivalent to fish mass, which is together with body size the common measure in fish
160 ecology, the relationship between individual body weight *w* (conventionally measured) and
161 body volume *v* (measured in the MRI) was analyzed.

162 For MR imaging of lipid distribution different approaches were taken into account before
163 starting the measurements. A search of the current literature on lipid quantification in fishes
164 revealed that, e.g., the Dixon technique, which is one of the state of the art techniques for
165 water-fat separation in medical research, yields unpersuasive results when applied to fishes
166 [20]. The contrast enhancement effect of lipid in fast spin echo sequences [21] (e.g. the rapid
167 acquisition with relaxation enhancement (RARE)) proved to be the most appropriate
168 approach and was chosen for the analysis of preserved samples. A standard multi-slice RARE
169 sequence protocol with the following parameters was used: TE= 14.9 ms, RARE factor: 4,
170 effective TEeff= 29.8 ms, TR= 5s, number of averages 30, 90° hermite pulse of 3 ms length,
171 180° hermite pulse of 1.9 ms, matrix 512x256, FOV 685x86,4 mm, 14-18 slices, slice
172 thickness 1.12 mm, total acquisition time 2h 40min.

173 After interpolation of the multi slice data sets to 3D matrices (minimum size 64/512/64
174 depending on fish length) percent overall lipid content was calculated from volume rendered
175 MRI scans using MeVis Lab in accordance with Machann and colleagues [22]. The lipid
176 content of individual *Pleuragramma* was calculated by converting the number of pixels into
177 a volume *v* [mm^3]. Bright pixels that arose from lipid-bound hydrogen atoms were separated
178 from other tissues using an operator-controlled threshold of 165 pixel units. The remaining
179 pixels were counted and summed up and finally divided from the overall sample volume. The
180 lipid content of individuals is then expressed by the percentage of lipid volume of total fish
181 body volume (i.e. lipid as % of total body volume).

182

183 The individuals of *Pleuragramma* that were used in this study are part of the institute's
184 collections and are too rare and valuable to be destroyed for a direct validation of these
185 results using chemical lipid extraction. Instead, previously published data on chemically
186 determined lipid content (and composition) of *Pleuragramma* sampled also in the Weddell
187 Sea were used to indirectly verify our measurements. For the comparison with these
188 literature data, which are usually given in % dry weight, a linear regression model based on
189 *Pleuragramma* tissue wet weights and dry weights analyzed as part of Mintenbeck and
190 colleagues [23] was used with a conversion factor of 0.154 to estimate initial dry weights of
191 the specimens used in this study.

192

193 **^{1}H-NMR spectroscopy and lipid composition**

194 Localized ^{1}H-NMR spectroscopy was conducted for the analysis of lipid composition, i.e. fatty
195 acid patterns in triacylglycerides [24, 25, 26]. Prior to spectroscopy, field homogeneity for
196 the specific volume of interest (voxel) was optimized using FASTMAP [27]. A standard ^{1}H
197 Point Resolved SpectroScopy (PRESS) sequence with the following parameters was used:
198 TE=21ms, TR = 5000ms, number of sampling points 2k, 256 averages, acquisition time 21m
199 40s. Individual voxels were placed inside specific regions of interest of the intermuscular
200 lipid layers according to previous acquired multi-slice MRIs (see above). Size of individual
201 voxel varied among samples and ranged from 3x3x3 to 2x2x8 mm, usually including 3-4 lipid
202 sacs within one voxel, resulting in a volume of interest between 27 and 32 mm^{3}. Localised
203 ^{1}H-MR spectra from lipids within the lipid sacs were measured in preserved individuals
204 sampled at two different locations in the Weddell Sea (Station A: area of the former Larsen A
205 ice shelf; Station B: area of the former Larsen B shelf ice). Prior to the main analysis, we
206 tested for within-fish and within-sampling location variability. There were no differences in

lipid composition within lipid sacs from different positions within one individual fish. Nevertheless, for the main analysis, the voxels for the localized MR spectroscopy in the lipid sacs were in each individual fish placed at the same position behind the first dorsal fin. The variability in lipid composition among individuals from one sampling location (Station A or B) was low.

Lipid composition was determined from the localized ^{1}H-MR spectroscopy using the approach recently described by Machann et al. [22]. The signals in the ^{1}H-NMR spectra were assigned to the respective triacylglyceride resonances according to Berglund et al. [26] and Petterson & Månsson [28].

Results and Discussion

General internal anatomy

The Antarctic silverfish *Pleuragramma antarctica* possesses some very special anatomical features such as the lipid sacs, the less ossified skeleton and the persistent gelatinous notochord [14, 17]. Images of this species are not (yet) part of the Digital Fish Library [5] and it was uncertain whether morphological data could be pictured in sufficient quality from preserved samples of this species due to the high total lipid content and the heterogeneous lipid distribution; both might theoretically induce artifacts in MR images due to susceptibility changes resulting from local inhomogeneity between different tissues and chemical shift effects between lipid and water. To test the applicability of MRI to preserved tissues of the Antarctic silverfish for the first time and to gain a first overview of the general internal anatomy, high-resolution 2D and 3D MR imaging, as proposed by Ziegler et al. [3], were applied.

Fig. 1 shows an example of a high-resolution morphological MR image of a multi-slice MR set. The excellent soft tissue contrast of the MR imaging technique allowed a clear distinction of muscle (M), notochord (N) and different organs such as brain (B), liver (Lv), and stomach (S) in the sagittal morphological section (Fig. 1A). There was no sign of any B0 or B1 inhomogeneity, indicating a very homogeneous excitation profile. Between outer skin and muscles, series of lipid sacs (ILS) can be identified in the dorsal part of the body along the back and in the ventral part of the body behind the abdomen (Fig. 1A). Fig. 1B shows a transversal MRI section taken from a 3D-morphological data set of a sample from this study in comparison to a histological cross (transversal) section of *Pleuragramma* from Eastman & DeVries [14] shown in Fig. 1C. Both transversal sections (Fig. 1B & C) are from the posterior one-fifth of the body of an adult individual [cf. 14, 17]. In the MRI slice muscle tissue is reflected in grey, whereas the lipids (ILS, SLS, IAT; Fig. 1B) generate a dark to almost no contrast. The details on the MR image are in well agreement with the histological image; even the thin collar of vertebral bone surrounding the notochord is visible. Besides of the large muscles, also the dorsal (DFM) and anal fin muscles (AFM) as shown in Johnston et al. [13] in histological sections (not shown here) can be identified on the MR image. Due to the lower resolution of MR images compared to histological images, very small details such as single muscle fibers or vacuoles and myocellular lipids [14, 17] can't be identified. However, despite of the lower resolution, the morphological imaging data sets obtained from non-destructive MRI technique provide almost the same array of information without the necessity to dissect and destroy the animal. In addition, despite of the high lipid content and heterogeneous structure, the MR images of preserved samples of *Pleuragramma* are of the same quality as, e.g., images from other (Antarctic) fish species such as *Notothenia corriiceps* as shown in the Digital Fish Library (see www.digitalfishlibrary.org).

As the lipid sacs in *Pleuragramma* are a rare feature among fish, their structure was studied in more detail. Within one particular fish and among individuals from the same sampling area, the shape of the single lipid sacs was similar. This was not the case among individuals from different areas. In Fig. 2 the high-resolution MRI scans of two individuals from different sampling regions are shown. The yellow boxes in both examples display almost identical positions within the fish. In the scan on the left, the lipid sacs are well separated from each other, while in the scan on the right the sacs are much more densely packed and display a much brighter image contrast (in particular within the yellow box). The reason for these differences still needs to be clarified. However, such morphological features of fragile objects like the lipid sacs get lost when using destructive techniques, but can be perfectly identified and analyzed in chemically preserved samples with non-invasive digital imaging approaches such as MRI.

Organ volume

Beside the representation of anatomic structures and details, the morphological MRI can produce 3D MR imaging data sets, e.g. from the abdominal region, which can be used to determine the volume of the specimen and specific organs of interest, such as the stomach (Fig. 3). The gastric wall exhibited a bright contrast in this MDEFT image set (see Fig. 3A-C), which could be easily separated from the other tissues using volume rendering tools (see Material & Methods). The rendered volume of one stomach is exemplarily shown in Fig. 3D. To show that the volume data measured in the MRI are comparable with conventional, ecological data, which are usually in units of weight (or size), the relationship between individual body weight (conventionally measured) and body volume (measured in the MRI) is shown in Fig. 4. According to these data, the relationship between both measures is almost

1:1 (y=0.998x, R^2=0.979), validating the comparability of body volume and body weight (i.e. 1 ml ≈ 1 g). Given that body volume *v* is a function of body weight *w* and body density *ρ* (*v*=*w*/*ρ*), the slope close to 1 is not surprising: *Pleuragramma* is almost neutrally buoyant, hence, its body density should be close to the density of the seawater, which on the high Antarctic shelf is about 1.03 g cm^{-3} (35 psu, -1,8°C). Accordingly, a body density *ρ* close to 1 g cm^{-3} can be expected for *Pleuragramma*, which means that for this species *v*≈*w*.

The volume of a stomach and the thickness of the gastric wall vary strongly depending on stomach fullness. Both, volume and wall thickness, are thus valuable indicators for the nutritional state of a fish and may be particularly useful for temporal or spatial comparisons of individuals in studies on a species' feeding habits. At present, in fish ecology, stomach fullness is determined gravimetrically or using rather subjective indices [29], both requiring dissection of the animals of interest and a lot of time.

Another important but time-consuming measure in fish ecology, beside stomach fullness, is the analysis of stomach content composition. Here, the limited gradient power (maximum of 200 mT/m) of the MR imaging system used in this study did not allow (with some exceptions) for identifying details of the stomach content. However, current animal scanners equipped with more powerful gradient systems of field strengths above 1000mT/m can easily reach an in plane resolution below 100 μm. Using such systems, the identification of particular prey organisms should be feasible (unless they are too heavily digested).

Here, the use of 3D MR imaging data sets for the determination of organ volumes was exemplified using stomachs of fish. The same methodology can be also applied to, e.g., the liver. In fish, the liver serves as an energy storage and is therefore smaller (and less heavy) in poor environments. Accordingly, in fish ecology, the ratio of liver to body weight (Hepatosomatic Index, HSI) is used as a measure of fish condition [30]. Intraspecific

comparison of liver volume using morphological MRI can therefore provide valuable information on conditions and prey availability in the area/season of capture.

Lipid content

Besides the excellent soft tissue contrast for morphological or anatomical observations, MR techniques can clearly separate tissue water from lipid and are frequently used for fat-water separation in medical research [for a review see 30]. Accordingly, MR techniques are frequently used for the analysis of body-fat content *in vivo* [10]. Recently, such MR analyses were also applied to fresh and defrosted fish tissue for an assessment of, e.g., food quality [20, 31, 32]. However, to our knowledge, these techniques to analyse body lipid content have never been applied to chemically preserved samples, before. As lipids in fish play an important role as energy reserve and in some species, such as *Pleuragramma*, also contribute to buoyancy, the proportion of lipids in the body is a measure of high interest in fish ecology. This particularly applies in the case of adult *Pleuragramma*, where the functional role of lipids is still under debate [18].

In species using lipids primarily as energy reserve, total body lipid content is significantly positively correlated to fish condition [33]. In *Pleuragramma* overall lipid content was shown to vary with fish body size and life cycle [34, 35, 36, 37]; in *Pleuragramma* larvae total lipid content was used as a marker for the nutritional condition [38].

In Fig. 5B, the blue areas show the lipid fractions depicted with volume rendering and contrast thresholds (see Material & Methods) from the RARE imaging data. The distribution of lipids obtained from the RARE images is in very well agreement with the distribution in the histological sections from Eastman [15, 17] and Eastman & DeVries [14]. Even the thin

lipid layer surrounding the vertebral thin collar and the notochord can be identified on the MR image (Fig. 5B). The notochord itself does not contain lipids (as shown by the lack of blue color). This is a clear improvement to the morphological data acquired with the MDEFT sequence, where the notochord and lipids were not clearly distinguishable (see Fig. 1B).

The total lipid content of *Pleuragramma*, as determined from the RARE scans, averaged 9.9 ± 1.7 % of wet weight (WW) and 51 ± 9 % of dry weight (DW; converted), respectively (n = 5; mean individual body weight: 15± 1 g WW; mean standard length, SL: 13.7 ± 0.2 cm). These results are in very good agreement with literature data on lipid content analyses based on chemical extraction from similar-sized *Pleuragramma* from the Weddell Sea (mean SL: 15.5 cm, mean lipid contents: 10.2 % WW and 47 % DW; see [34]) and demonstrate the suitability of RARE imaging for lipid determination in preserved fish samples.

Lipid composition

Triacylglycerides and wax esters are the most common lipid classes in marine organisms including fish. Both lipid classes are used as energy reserve and buoyancy aid. Lipid composition of fish is influenced by the diet, because the fatty acid profile of a consumer reflects the fatty acids of its prey and its nutrition value [39, 40, 41]. Accordingly, lipid class composition and fatty acid signatures are commonly used markers to analyze consumers' trophic ecology [42, 43, 44]. Recently, it has been shown that the lipid composition of adipose tissue and lipid stores can be determined in humans and mammals using localized ^{1}H-NMR spectroscopy (see Material & Methods). The ratios of the ^{1}H-NMR signals of the fatty acids can be used for the calculation of mean chain length, unsaturation status and the mono- and poly-unsaturation fractions of triacylglycerides, as shown for instance by

348 Berglund et al. [26]. Here, localized ^{1}H-NMR spectroscopy was applied to analyze the
349 composition of lipids stored in the intermuscular sacs (ILS) of *Pleuragramma*.

350 Figure 6 presents the localized ^{1}H-NMR spectra from two individuals sampled at two
351 different locations in the Weddell Sea (Station A and Station B, see Material and Methods for
352 details). The measured spectra show a typical lipid pattern and the particular signals could
353 be assigned to hydrogen atoms bound in specific positions of fatty acids according to the
354 literature [22, 24, 2454]. The signal intensities reflect the relative concentration of hydrogen
355 atoms bound to specific lipid groups and the signal of the CH_3-group can be used as an
356 internal standard for calibration [22]. According to the spectra in Fig. 6 the dominating lipid
357 class in the lipid sacs of *Pleuragramma* is triacylglyceride, which is in accordance with results
358 on muscle tissue and overall lipid content determined using classical chemical lipid analyses
359 [11, 45, 46]. Interestingly, distinct differences are also obvious between both spectra: e.g.
360 the signals from the -(CH_2)- and the -CH_2-CH=CH-CH_2- group are much more pronounced in
361 the individual from Station A in Fig. 6. These differences are confirmed by the detailed
362 results from the ^{1}H-NMR spectra summarized in Table 1. While the average chain length was
363 similar in individuals from both sampling stations (A & B), the lipids of individuals from the
364 two locations significantly differed in their unsaturated and polyunsaturated degree
365 ($p<0.05$). Though the actual causes for these differences remain unsolved, so far, such
366 differences might indicate potential functional changes within the lipid sacs induced by
367 specific changes in energy/lipid metabolism of the organism.

368 Because of the fragile nature of the lipid sacs, an analysis of localized lipid composition
369 inside the structures seems almost impossible using traditional, destructive methods. Here,
370 the composition inside this particular lipid storage system was analysed for the first time
371 using ^{1}H-NMR spectroscopy.

To be considered when working with preserved samples

All kinds of sample preservation affect tissues of organisms in one or the other way. Potential effects differ among preservation method and may involve, e.g., alterations in biochemical composition, shrinkage due to water extraction or cell disruption. Formalin and its derivates may induce changes in size and weight, as shown for instance in mice brain [46]. Formalin fixation thus may result in an underestimation of measured organ volume of a preserved sample, though the reported changes are only in the range of a few percentages. Formalin (as well as methanol) may cause hydrolysis of tissue lipids and degradation of polyunsaturated fatty acids and phospholipids [48, 49], while neutral lipids are obviously not affected [50]. Most changes apparently occur during a short time frame directly after exposure to the preservation medium, within the first few hours or days; during this period, measurements and analyses of preserved samples should be avoided [51]. In some studies no significant effect of formalin on biochemical composition of tissue and samples, respectively, was found [52, 53]; other studies considered a potential effect negligible, at least as long as the lipid containing tissues are intact [54, 55].

In the present study, whole, undamaged animals were used, without any defects in the skin that might have facilitated leakage of lipids from the lipid sacs. The MRI studies were started about one year after fixation in 10% buffered formalin and repeated in part after another year of formalin storage. No significant difference in weight, volume or shape could be detected between the two time points, nor was there a difference in measured total lipid content (personal observation). The risk of lipid loss is expected to be increased in tissues samples (e.g. liver) that are directly exposed to the preservative. Whole organisms, with intact intestines and tissues, are most likely less affected. However, some formalin-induced

short term release of e.g. phospholipids can't be completely excluded. As lipids in *Pleuragramma* are mainly represented by neutral triacylglycerides (in particular inside the lipid sacs) while the amount of phospholipids is very low [37, 46], a potential effect of the preservation on overall lipid content and composition is considered negligible, here; in particular because treatment, preservation and storage were identical for all individuals. Nevertheless, for future MRI studies such potential effects of the preservation methods needs to be taken into account, particularly when different preservation methods are used or preserved samples are compared to fresh material.

Conclusions

As shown in this study, MRI and MRS on preserved fish samples may not only contribute anatomical and morphometric 3D data to digital libraries and atlantes, but also provide valuable insights into functional morphology (organ volumes, lipid distribution), energetics (lipid content) and biochemical composition (lipid composition). Using MRI, lipid content and organ volumes can be reliably determined. Unexpected and unknown differences in the shape of lipid sacs among individuals, that would have been hardly found using traditional methods, could be detected. ^{1}H-NMR spectroscopy proved to be a valuable tool to analyze lipid composition, which usually requires destruction of the animal and complex chemical lipid exaction and analysis. The localized spectroscopy allowed for the first analysis of lipid composition inside the lipid sacs and revealed differences in lipid composition among individuals from different sampling stations.

Lipid distribution, content and composition as well as organ volumes are all parameters of high ecological relevance. For the study of preserved samples, MRI and MRS proved to be a

highly valuable addition, if not alternative, to the classical methods. The advantage that these modern techniques are non-invasive and non-destructive opens an array of opportunities for studies of preserved samples from natural history museums' collections.

Acknowledgements

We like to thank Prof. Dr. Rascher-Friesenhausen for providing a MeVis Lab software licence and the crew and officers of FS Polarstern during ANTXXVII/3 for their professional support. We also acknowledge the American Society of Ichthyologists and Herpetologists (ASIH), in particular the Editor of Copeia, Christopher Beachy, for granting permission to reprint Fig. 2A from Eastman & DeVries [14] (Fig. 1C in this manuscript). Two anonymous reviewers provided helpful comments on an earlier version of the manuscript. This work including animal sampling and analyses were funded by the German Research Foundation (DFG, SSP 1158), grant MI 1391/1-1.

References

[1] Baker M. (2010) The whole picture. Nature. 463: 977-980.

[2] Lauridsen H, Hansen K, Wang T, Agger P, Andersen JL, Knudsen PS, Rasmussen AS, Uhrenholt L, Pedersen M (2012) Inside out: modern imaging techniques to reveal animal anatomy. PloS One 6: e17879.

[3] Ziegler A, Kunth M, Mueller S, Bock C, Pohmann R, Schröder L, Faber C, Giribet G (2011) Application of magnetic resonance imaging in zoology. Zoomorphology 130: 227-254.

[4] Simões JM, Teles MC, Oliveira RF, Van den Linden A, Verhoye M (2012) A three-dimensional stereotaxic MRI brain atlas of the cichlid fish Oreochromis mossambicus. PLoS One 7: e44086.

[5] Berquist RM, Gledhill KM, Peterson MW, Doan AH, Baxter GT, Yopak KE, Kang N, Walker HJ, Hastings PA, Lawrence RF (2012) The digital fish library: using MRI to digitize, database, and document the morphological diversity of fish. PLoS One 7: 1-16.

[6] Ziegler A, Faber C, Mueller S, Bartolomaeus T (2008) Systematic comparison and reconstruction of sea urchin (Echinoidea) internal anatomy: a novel approach using magnetic resonance imaging. BMC Biol 6: 33.

[7] Bock C, Frederich M, Wittig RM, Pörtner HO (2001) Simultaneous observations of haemolymph flow and ventilation in marine spider crabs at different temperatures: a flow weighted MRI study. Magn Reson Imaging 19: 1113-1124.

[8] Orgiu S, Lafortuna CL, Rastelli F, Cadioli M, Falini A, Rizzo G (2015) Automatic muscle and fat segmentation in the thigh from T1-weighted MRI. J Magn Reson Imaging. DOI: 10.1002/jmri.25031.

463 [9] Van der Linden A, Verhoye M, Pörtner HO, Bock C (2004) The strengths of in-
464 vivo Magnetic Resonance Imaging (MRI) to study environmental adaptational
465 physiology in fish. MAGMA 17: 236-248.
466 [10] Chatham JC, Blackband SJ (2008) Nuclear magnetic resonance spectroscopy
467 and imaging in animal research. ILAR J 42: 189-208.
468 [11] DeVries AL, Eastman JT (1978) Lipid sacs as a buoyancy adaptation in an
469 Antarctic fish. Nature 271: 352-353.
470 [12] Eastman JT (1988a) Ocular morphology in antarctic notothenioid fishes. J
471 Morphol 196:283-306.
472 [13] Johnston IA, Camm J-P, White M (1988) Specialisations of swimming muscles
473 in the pelagic Antarctic fish *Pleuragramma antarcticum*. Mar Biol 100: 3-12.
474 [14] Eastman JT, DeVries AL (1982) Buoyancy studies of notothenioid fishes in
475 McMurdo Sound, Antarctica. Copeia 2: 385-393.
476 [15] Eastman JT (1985) The evolution of neutrally buoyant notothenioid fishes:
477 Their specialization and potential interactions in the Antarctic marine food web. In:
478 Siegfried WR, Condy PR, Laws RM, editors. Antarctic Nutrient Cycles and Food Webs.
479 Springer Berlin Heidelberg. Pp. 430-436.
480 [16] Eastman JT (1997) Phyletic divergence and specialization for pelagic life in the
481 Antarctic nototheniid fish *Pleuragramma antarcticum*. Comp Biochem Physiol 118A:
482 1095-1101.
483 [17] Eastman JT (1988b) Lipid storage systems and the biology of two neutrally
484 buoyant Antarctic Notothenioid fishes. Comp Biochem Physiol 90B: 529-537.
485 [18] Maes J, Van de Putte A, Hecq JH, Volckaert FAM (2006) State-dependent
486 energy allocation in the pelagic Antarctic silverfish *Pleuragramma antarcticum*:

trade-off between winter reserves and buoyancy. Mar Ecol Prog Ser 326: 269-282.

[19] Knust R, Gerdes D, Mintenbeck K, editors (2012) The Expedition ANTARKTIS XXVII/3 CAMBIO) of RV "Polarstern" in 2011. Rep Polar Mar Res 644. 200pp.

[20] Brix O, Apablaza P, Baker A, Taxt T, Grüner R (2009). Chemical shift based MR imaging and gas chromatography for quantification and localization of fat in Atlantic mackerel. J Exp Mar Biol Ecol 2009;376(2):68–75.

[21] Henkelman RM, Hardy PA, Bishop JE, Poon CS, Plewes DB (1992). Why fat is bright in RARE and fast Spin-Echo imaging. J Magn Reson Imag 2: 533-540.

[22] Machann J, Stefan N, Schabel C, Schleicher E, Fritsche A, Würslin C, Häring H-U, Claussen CD, Schick F (2012) Fraction of unsaturated fatty acids in visceral adipose tissue (VAT) is lower in subjects with high total VAT volume – a combined 1H MRS and volumetric MRI study in male subjects. NMR Biomed 26: 232-236.

[23] Mintenbeck K, Brey T, Jacob U, Knust R, Struck U (2008) How to account for the lipid effect on carbon stable-isotope ratio /d13C): sample treatment effects and model bias. J Fish Biol 72: 815-830.

[24] Ye Q, Danzer CF, Fuchs A, Vats D, Wolfrum C, Rudin M (2012) Longitudinal evaluation of hepatic lipid deposition and composition in ob/ob and ob/+ control mice. NMR Biomed 29: 1079-1088.

[25] Lee Y, Jee H-J, Noh H, Kang G-H, Park J, Cho J, Cho J-H, Ahn S, Lee C, Kim O-H, Oh B-C, Kim H (2013) In vivo 1H-MRS hepatic lipid profiling in nonalcoholic fatty liver disease: An animal study at 9.4 T. Magn Reson Med 70: 620-629.

[26] Berglund J, Ahlström H, Kullberg J (2012) Model-based mapping of fat unsaturation and chain length by Chemical Shift Imaging – phantom validation and in vivo feasibility. Magn Reson Med 68: 1815-1827.

511 [27] Gruetter R (1993). Automatic, localized *in vivo* adjustment of all first and
512 second-order shim coils. Magn Reson Med 29:804-811.
513 [28] Petterson P, Månsson S (2013) Simultaneous quantification of fat content and
514 fatty acid composition using MR imaging. Magn Reson Med 69: 688-697.
515 [29] Dalpado P, Gjøsæter J (1988) Feeding ecology of the laternfish *Benthosema*
516 *pterotum* from the Indian Ocean. Mar Biol 99: 555-567.
517 [30] Lloret J, Gil de Sola L, Souplet A, Galzin R (2002) Effects of large-scale habitat
518 variability on condition of demersal exploited fish in the north-western
519 Mediterranean. ICES J Mar Sci 59: 1215-1227.
520 [31] Toussaint C, Fauconneau B, Médale F, Collewet G, Akoka S, Haffray P, Davenel
521 A (2005) Description of the heterogeneity of lipid distribution in the flesh of brown
522 trout (Salmo trutta) by MR imaging. Aquaculture 243: 255-267.
523 [32] Picaud J, Collewet G,*, Idier J. (2016). Quantification of mass fat fraction in
524 fish using water-fat separation MRI. Magn Reson Imag 34: 44-50.
525 [33] Herbinger CM, Friars GW (1991) Correlation between condition factor and
526 total lipid content in Atlantic Salmon, *Salmo salar* L., parr. Aquacult Fish Manage 22:
527 527-529.
528 [34] Friedrich C., Hagen W. (1994). Lipid contents of five species of notothenioid
529 fish from High-Antarctic waters and ecological implications. Polar Biol 14: 359–369.
530 [35] Hagen W, Kattner G, (2013). The role of lipids in the Antarctic silverfish
531 *Pleuragramma antarcticum*. Book of abstracts; XIth SCAR biology symposium. 15-
532 19.07.13, Barcelona, Spain, P-2.10: 224.
533 [36] Mayzaud P, Chevallier J, Tavernier E, Moteki M, Koubbi P (2011) Lipid
534 composition of the Antarctic fish *Pleuragramma antarcticum*. Influence of age class.

535 Polar Sci 5: 264-271.
536 [37] Reinhardt SB, van Vleet ES (1985) Lipid composition of Antarctic midwater
537 fish. Ant J US 19:144-145.
538 [38] Giraldo C, Mayzaud P, Tavernier E, Irisson J-O, Penot F, Becciu J, Chartier A,
539 Boutoute M, Koubbi P (2013) Lipid components as a measure of nutritional condition
540 in fish larvae (*Pleuragramma antarcticum*) in East Antarctica. Mar Biol 160: 877-887.
541 [39] Kamler E, Krasicka B, Rakusa-Suszczewski S (2001) Comparison of lipid content
542 and fatty acid composition in muscle and liver of two notothenioid fishes from
543 Admiralty Bay (Antarctica): an eco-physiological perspective. Polar Biol 24:735-743.
544 [40] Lea M-A, Nichols PD, Wilson G (2002) Fatty acid composition of lipid-rich
545 myctophids and mackerel icefish (*Champsocephalus gunnari*) - Southern Ocean
546 food-web implications. Polar Biol 25: 843-845.
547 [41] Phleger CF, Nelson MM, Mooney BD, Nichols PD (1999) Wax esters versus
548 triacylglycerols in myctophid fishes from the Southern Ocean. Antarct Sci 11: 436-
549 444.
550 [42] Iverson S J, Field C, Bowen WD, Blanchard W (2004) Quantitative fatty acid
551 signature analysis: A new method of estimating predator diets. Ecol Monogr 74: 211-
552 235.
553 [43] Nyssen F, Brey T, Dauby P, Graeve M (2005) Enhanced analysis of trophic
554 position of Antarctic amphipods revealed by a 2-dimensional biomarker assay. Mar
555 Ecol Prog Ser 300: 135-145.
556 [44] Alfaro AC, Thomas F, Sergent L, Duxbury M (2006) Identification of trophic
557 interactions within an estuarine food web (northern New Zealand) using fatty acid
558 biomarkers and stable isotopes. Estuar Coast Shelf Sci 70: 271-286.

559 [45] Hubold G, Hagen W (1997) Seasonality of feeding and lipid content of
560 *Pleuragramma antarcticum* (Nototheniidae) in the southern Weddell Sea. In:
561 Battaglia B, Valencia J, Walton DWH, editors. Antarctic communities: species,
562 structure and survival. Cambridge University Press, Cambridge. Pp. 277-283.
563 [46] Hagen W, Kattner G, Friedrich C (2000) The lipid compositions of high-
564 Antarctic notothenioid fish species with different life strategies. Polar Biol 23: 785-
565 791.
566 [47] Weisbecker V (2012) Distortion in formalin-fixed brains: using geometric
567 morphometrics to quantify the worst-case scenario in mice. Brain Struct Funct 217:
568 677-685.
569 [48] Morris RJ (1972) The preservation of some oceanic animals for lipid analysis. J
570 Fish Res Board Can 29: 1303-1307.
571 [49] Halliday N (1939) The effect of formalin fixation on liver lipids. J Biol Chem
572 129: 65-69.
573 [50] Kapiris K, Miliou H, Moraitou-Apostolopoulou M (1997) Effects of
574 formaldehyde preservation on biometrical characters, biomass and biochemical
575 composition of *Acartia clause* (Copepoda, Calanoida). Helgolander Meeresun 51: 95-
576 106.
577 [51] Steedman HF, editor (1976) Zooplankton fixation and preservation. The
578 Unesco Press, Paris. 350p.
579 [52] Danovaro R, Dell'Anno A, Martorano D, Parodi P, Marrale ND, Fabiano M
580 (1999) Seasonal variation in the biochemical composition of deep-sea nematodes:
581 bioenergetic and methodological considerations. Mar Ecol Prog Ser 179: 273-283.
582 [53] Wakeham SG, Hedges JI, Lee C, Pease TK (1993) Effects of poisons and

583 preservatives on the composition of organic matter in a sediment trap experiment. J
584 Mar Res 51: 669-696.
585 [54] Davies KTA, Ryan A, Taggart CT (2012) Measured and inferred gross energy
586 content in diapausing *Calanus* spp. in a Scotia shelf basin. J Plankton Res 34: 614-
587 625.
588 [55] Heulett ST, Weeks SC, Meffe GK (1995) Lipid dynamics and growth relative to
589 resource level in juvenile Eastern Mosquitofish (*Gambusia holbrooki*: Poeciliidae).
590 Copeia 1: 97-104.
591
592
593
594

Figure legends:

Figure 1: Example of a high-resolution morphological MRI scan obtained from a formalin preserved sample of *Pleuragramma* using MDEFT. The figure shows a sagittal section (A) and a transversal (cross) section (B) of an individual analyzed in this study in comparison to (C) a histological transversal section of *Pleuragramma* from Eastman & DeVries [14] (with kind permission from Copeia and the American Society of Ichthyologists and Herpetologists, ASIH). B, brain; IAT, intermuscular adipose tissue; ILS, intermuscular lipid sacs (dorsal and ventral); Lv, liver; M, muscle; N, notochord; NV, notochordal vesicles; RMLS, red muscle fibres of the lateralis superficialis (according to Eastman & DeVries [14]); S, stomach; SLS, subcutaneous lipid sacs; DFM, dorsal fin muscles and AFM, anal fin muscles according to Johnston et al. [13].

Figure 2: Magnification of high-resolution MRI scans (MDEFT) of the dorsal lipid sac region from two different *Pleuragramma* individuals sampled at different areas. Note the different shape of the lipid sacs between both examples (see yellow boxes).

Figure 3: Examples of 3D MR image sets (MDEFT) taken in the abdominal region of preserved *Pleuragramma*. Shown are a sagittal (A), a coronal (B) and a transversal section (C). On the right, the 3D surface-rendered stomach (D), as used for volume determination, is shown.

Figure 4: Relationship between individual body weight [g] and body volume [ml] in *Pleuragramma* (N=6). Dashed line represents the linear relationship described by $y=0.997x$ ($R^2=0.98$). Note the excellent correlation that allows a direct conversion from volume into weight.

Figure 5: Example of a whole body 3D MRI data set acquired with RARE of *Pleuragramma* used for the analysis of body lipid content. In (A) a sagittal, a coronal and a transversal section are shown; lipids are bright/white, other tissues are grey. In (B) an example of a transversal MRI after volume rendering is shown, illustrating the muscle/water (grey) and lipid (blue) distribution in *Pleuragramma*.

Figure 6: ^{1}H-NMR spectra measured in the dorsal intermuscular lipid sacs (ILS) of two different individual fish from two sampling locations (Stations A and B). The ROI (volume from where the spectrum was acquired) are marked by the red square. Both NMR spectra display a “typical” triacylglyceride/lipid pattern, but show clear differences in specific signal intensities.

Figure 1

Click here to download high resolution image

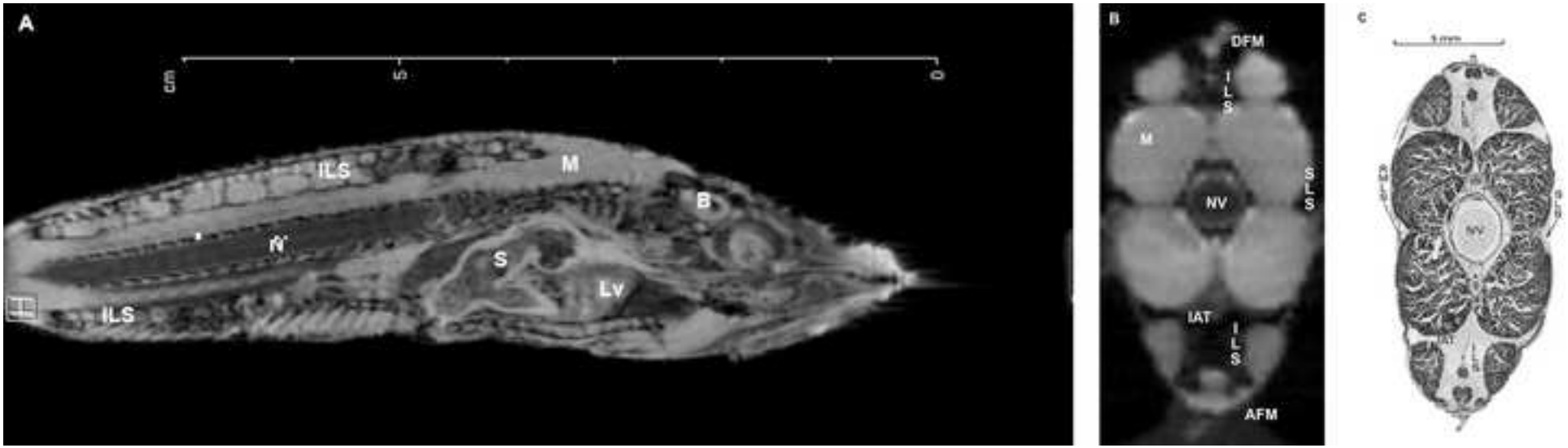

Figure 2

Click here to download high resolution image

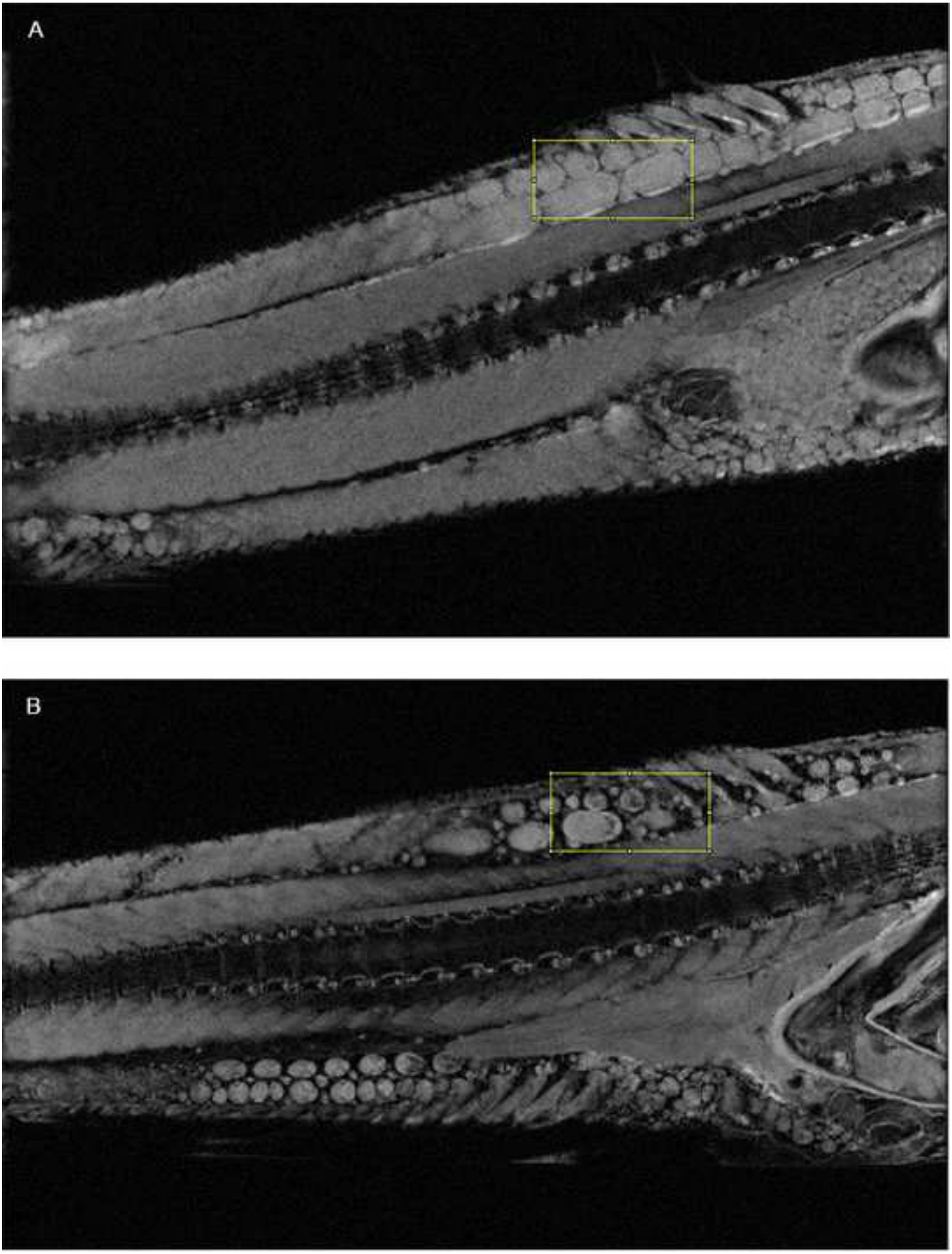

Figure 3

Click here to download high resolution image

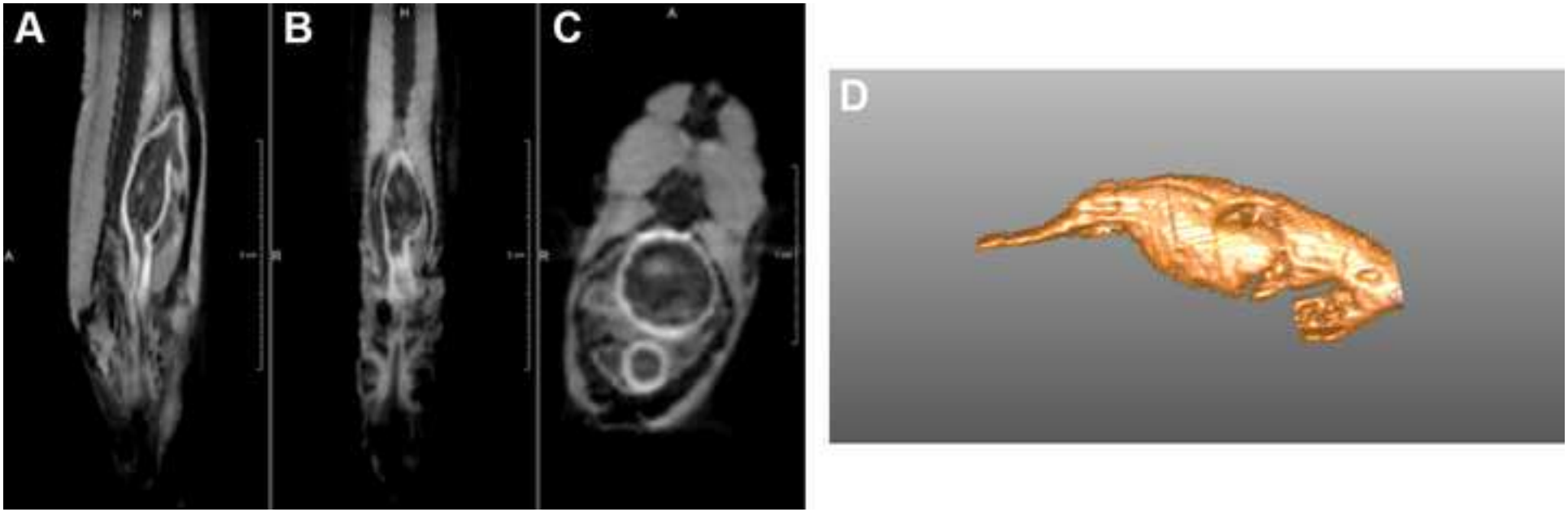

Figure 4

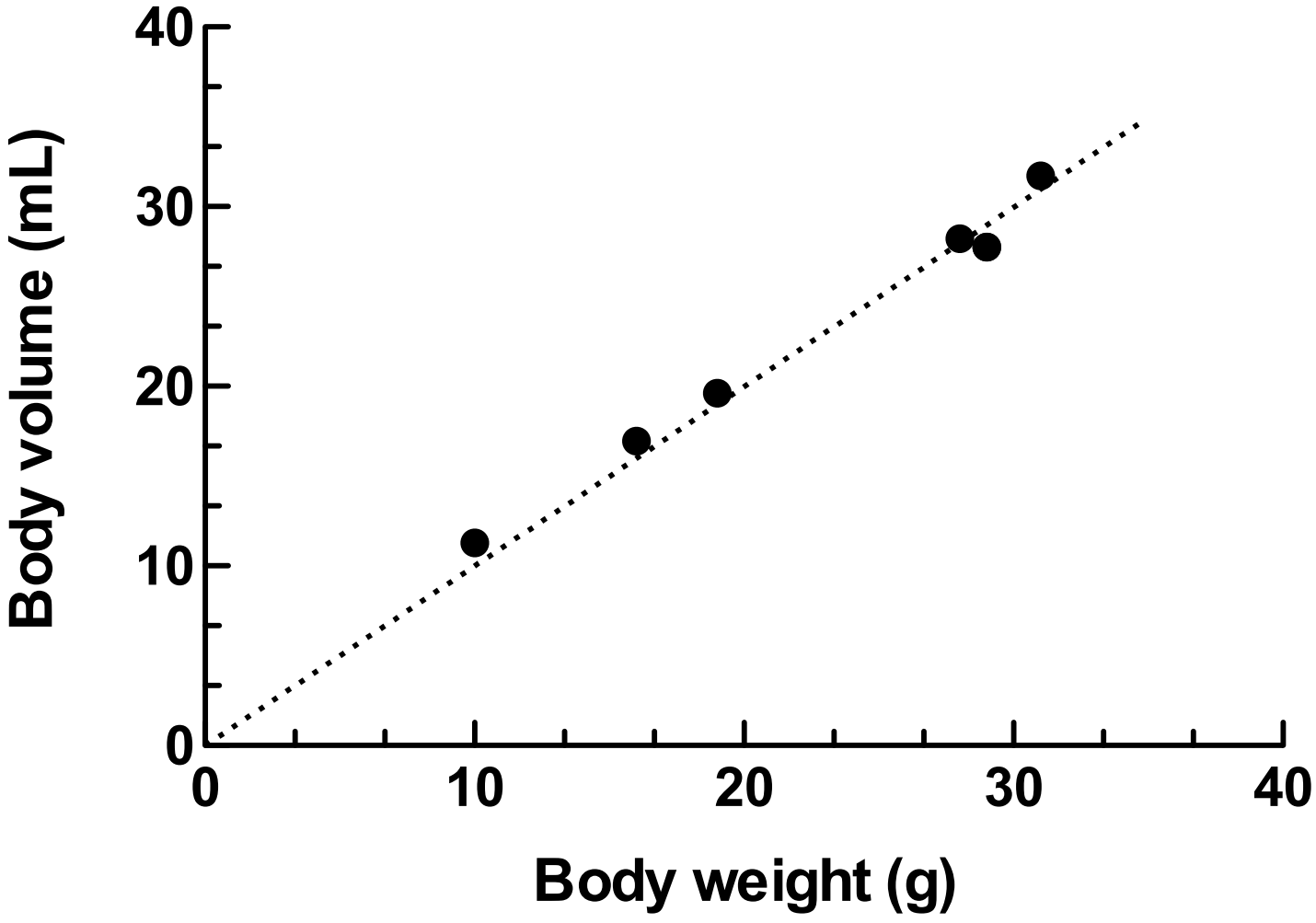

Figure 5

Click here to download high resolution image

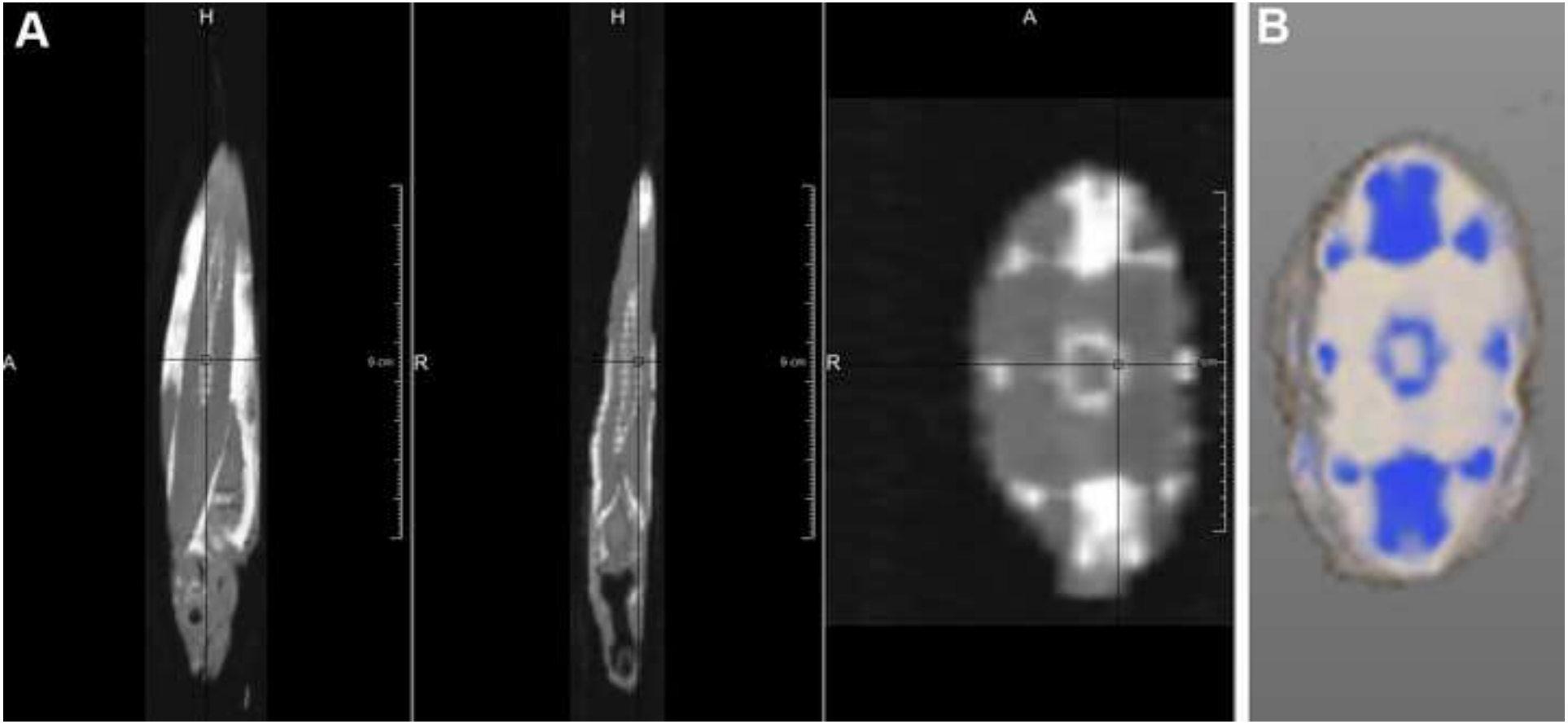

Figure 6mod

Click here to download high resolution image

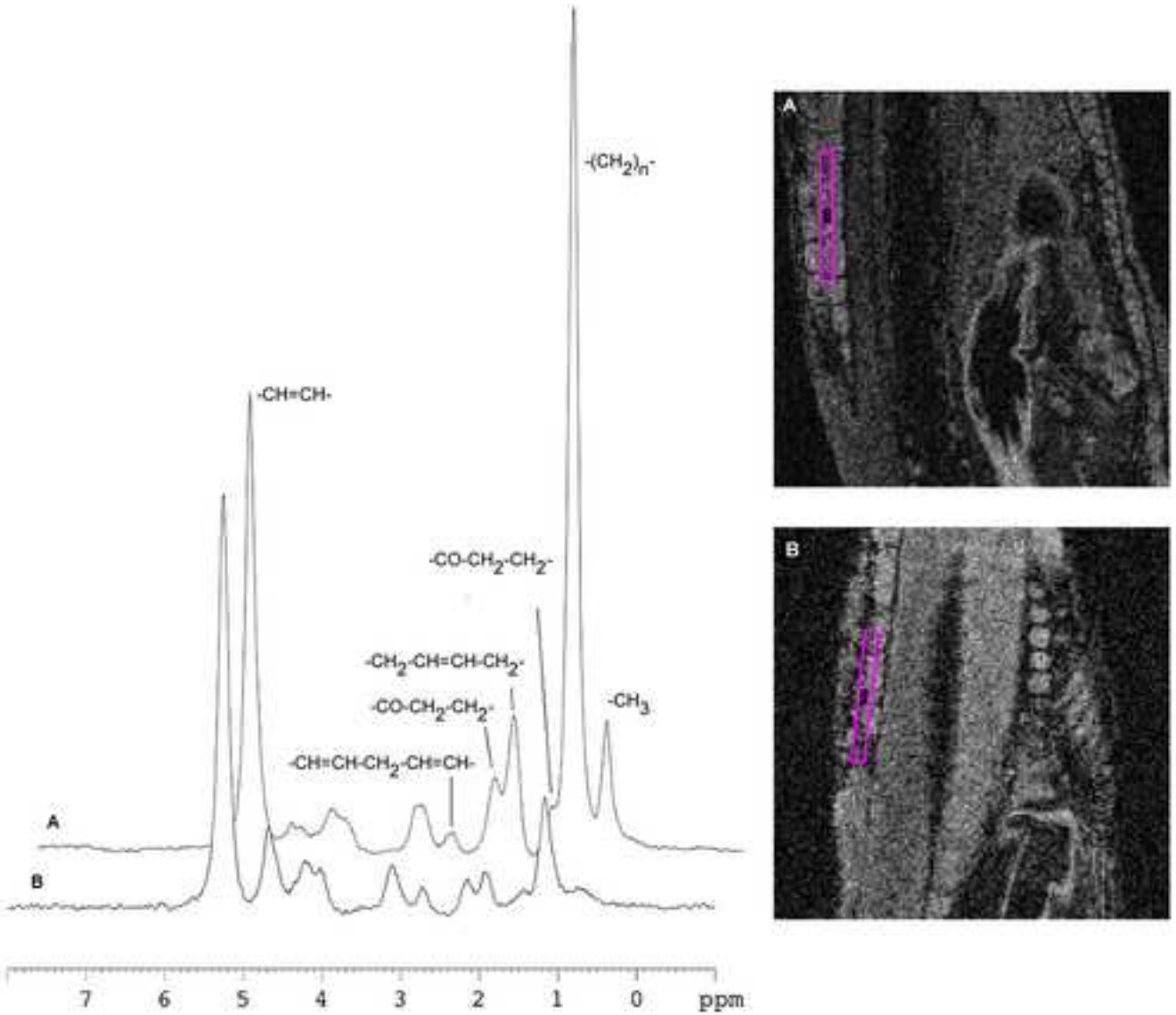

Table 1: Mean fatty acid (FA) chain length, unsaturation degree and degree of poly-unsaturation derived from localized ^{1}H-NMR spectra measured within the intermuscular lipid sacs of preserved fish from two different sampling locations, Station A (area of the former Larsen A shelf ice) and Station B (former Larsen B shelf ice).* significantly different from Station A, $p<0.05$.

	FA chain length	Unsaturation degree	Polyunsaturation degree
Station A (n=4)	7,98±1,98	3,15±1,68	1,45±0,79
Station B (n=5)	6,06±1,14	1,21±0,79*	0,36±0,26*